

Structural Role of Water in a Sodium Phosphate Glass by Neutron Diffraction

U. Hoppe, R. Kranold, D. Stachel^a, A. Barz^a, and C. J. Benmore^b

Universität Rostock, Institut für Physik, D-18051 Rostock

^a Otto-Schott-Institut für Glaschemie, Friedrich-Schiller-Universität Jena, D-07743 Jena

^b ISIS Facility, Rutherford Appleton Laboratory, Chilton, Didcot OX11 0QX, UK

Present address: Intense Pulsed Neutron Source, Argonne National Laboratory, IL 60439, USA

Reprint requests to Dr. U. H.; Fax: +49 381 4986862, E-mail: Hoppe@physik1.uni-rostock.de

Z. Naturforsch. **59a**, 879–887 (2004); received September 17, 2004

Neutron diffraction with isotopic H/D-substitution was used to study the network-modifying effect of water in a $\text{H}_2\text{O}-\text{Na}_2\text{O}-2\text{P}_2\text{O}_5$ glass. The resolved fractions of P–O_T and P–O_B bonds and the O–O coordination number indicate similarity to the specifics of a metaphosphate structure. Thus, oxygen of H_2O added ruptures a P–O–P bridge, increasing the number of terminal oxygens. The combined analysis of the first-neighbour peaks in the correlation functions of the hydrogenated and deuterated samples yields H–O distances of 0.101 and 0.157 nm and H–P distances of 0.223 and 0.250 nm. Such distances are well explained with the formation of O–H···O hydrogen bridges. The corresponding O–O distances superpose with the edge lengths of the PO_4 tetrahedra. Significant fractions of short H–H distances typical of water molecules (0.155 nm) or clustering of hydrogen bridges are not detected. The Na–O coordination number of five is similar to that found for the NaPO_3 glass.

Key words: Isotopic Substitution; Neutron Scattering; Hydrogen Bridges; Phosphate Glasses.

1. Introduction

Vitreous P_2O_5 and phosphate glasses rich in P_2O_5 content are sensitive to humidity [1]. Water molecules attacking the glass structure act as network modifiers by rupturing the P–O–P bridges. This behaviour has been demonstrated by infrared (IR) spectroscopy [2] and by ^{31}P magic angle spinning nuclear magnetic resonance (MAS NMR) spectroscopy [3]. The hydrogen atoms form single covalent bonds with the terminal oxygens (O_T) and, additionally, are expected to approach another O_T of a second PO_4 tetrahedron to realize hydrogen bond forming O–H···O bridges. The verification of this behaviour by diffraction methods is difficult. Hydrogen atoms are weak scatterer for photons in x-ray diffraction (XRD) experiments. Nevertheless, the H^+ positions in structures of related ultra- and polyphosphate crystals have been determined by XRD [4–7]. Neutron scattering (ND) is a better tool for structural analysis of systems containing hydrogen. But scattering of the neutrons by the light protons (H^+) causes strong repulsion effects. The required inelasticity corrections are very difficult [8]. Furthermore, the interesting coherent scattering part

of hydrogen is only 2% of its total scattering cross-section [9]. Thus, a serious background of unknown behaviour affects the measured differential scattering cross-sections which bears uncertainties especially to the analysis of scattering data of disordered systems. The problems are clearly reduced with a substitution of hydrogen by deuterium, which causes a smaller fraction of incoherent scattering [9] with smaller repulsion effects. On the other hand, the comparison of the coherent scattering length of H (–3.74 fm) with that of D (6.67 fm) [9] suggests to perform contrast variation experiments. The critical point is still the inelasticity correction whose uncertainty, however, can be reduced applying special experimental conditions such as the use of only small scattering angles. This is possible using epithermal neutrons up to energies of $E \cong 4$ eV. The SANDALS instrument at the neutron spallation source ISIS (Chilton/UK) is optimized for such experiments [10]. In this work we want to apply this instrument, using H/D-substitution to study water incorporation into glassy phosphate networks. The ^{31}P MAS NMR results of sodium ultraphosphate glasses prepared in standard procedure with open crucibles have shown that only $\text{H}_2\text{O}-\text{Na}_2\text{O}-\text{P}_2\text{O}_5$ glasses

close to the metaphosphate composition with dominance of twofold-connected PO_4 middle groups are obtained [3]. The mole content of water in the resulting glasses can even exceed the Na_2O modifier content. The samples for the present study will have a similar composition with equimolar fractions of Na_2O and $\text{H}_2\text{O}(\text{D}_2\text{O})$ in a metaphosphate glass (50 mol% P_2O_5). In order to prevent any change of the water content during melting the materials have to be prepared in sealed ampoules. Originally, this preparation method was developed to obtain anhydrous glasses with high P_2O_5 contents [2]. Two samples with equal content of water are prepared which differ using either H_2O or D_2O . A difference structure factor $\Delta S(Q)$ obtained from the resulting total structure factors, $S_{\text{H}}(Q)$ and $S_{\text{D}}(Q)$, will only show information of the H–O, H–P, H–Na and H–H pair correlations. Similar experiments have been made on sodium silicate glasses containing up to 25 mol% H_2O [11]. Clear H–O peaks were detected at 0.10 nm [11]. Other pair distances in the difference correlation function $\Delta T(r)$ obtained from $\Delta S(Q)$ follow for $r > 0.25$ nm with a peak at 0.3 nm [11]. They belong to H–Si, H–Na and also to longer H–O separations. Beside OH-groups, also considerable fractions of H_2O in molecular form were detected by IR spectroscopy [11]. H_2O molecules should not exist in the phosphate glasses studied [3].

2. Experimental

2.1. Sample Preparation

Anhydrous NaPO_3 and P_4O_{10} were mixed in appropriate quantities with $\text{H}_2\text{O}(\text{D}_2\text{O})$ and loaded in silica ampoules before evacuating and sealing them. The duration of melting at 1000 °C was 30 min with subsequent annealing at 300 °C. For both glasses second ampoules were prepared and broken for the determination of compositions and mass densities. The Na and P contents were measured photometrically. H_2O and D_2O contents were obtained from the difference to the total mass. All differences between the analysed and nominal compositions were less than 1 mole%. Mass densities of 2.45 and 2.43 g/cm³ were found for the hydrogenated and deuterated samples, respectively. Hence, it is justified to use the nominal compositions and a mass density of 2.44 g/cm³ for the subsequent structural analysis. A number density of atoms of 80.5 nm^{−3} corresponds to the mass density.

2.2. Neutron diffraction experiments

The sample material was crushed to a coarse-grained powder and loaded into slab-shaped cans of 35×38 mm² area, greater than the beam size with a diameter of 32 mm, whereby a glove box was used for the preparations. The cans had an internal width of 2 mm. Their window material was Ti/Zr alloy of zero coherent scattering. A vanadium slab of 3.5 mm thickness was used to obtain the energy spectrum of the neutron source. The sample runs had a duration of 12 h. The detector groups of SANDALS cover scattering angles 2θ from 3.8° to 39°. So it is possible to reach magnitudes of the scattering vector up to $Q \geq 300$ nm^{−1}. The corrections for absorption, multiple scattering and background were performed for the data of each of the 18 detector groups separately, using the ATLAS program suite [12]. The data were normalized to the vanadium standard. The self-scattering terms $(d\sigma/d\Omega)_{\text{self}}$, which decrease smoothly with increasing Q , were fitted with Chebyshev polynomials by the routine SUBSELF. The maximum degree of polynomial and a minimum radius of physically possible pair distances are parameters of the fit. The radii used were 0.05 and 0.02 nm for the hydrogenated (HNaP) and deuterated (DNaP) samples. Finally, the distinct scattering terms $(d\sigma/d\Omega)_{\text{dis}}$ were obtained from the normalized differential scattering cross-sections with

$$(d\sigma/d\Omega)_{\text{dis}} = (d\sigma/d\Omega) - (d\sigma/d\Omega)_{\text{self}}, \quad (1)$$

and have been merged subsequently. The total structure factors are calculated with

$$S(Q) = (d\sigma/d\Omega)_{\text{dis}} / \langle b \rangle^2 + 1, \quad (2)$$

where $\langle b \rangle$ is the sample average of the coherent scattering lengths.

In order to examine the quality of the $S(Q)$ data a short run with the deuterated sample was made on the LAD instrument and a short run with the NaPO_3 glass just before measured on LAD was made on SANDALS. The LAD results of the two anhydrous sodium phosphate glasses with 37.9 and 50 mole% Na_2O are reported in [13], where also the corresponding experimental conditions are described.

3. Results

The experimental structure factors, $S_{\text{H}}(Q)$ and $S_{\text{D}}(Q)$, of the HNaP and DNaP samples are compared in Fig. 1 together with the $S(Q)$ factors of

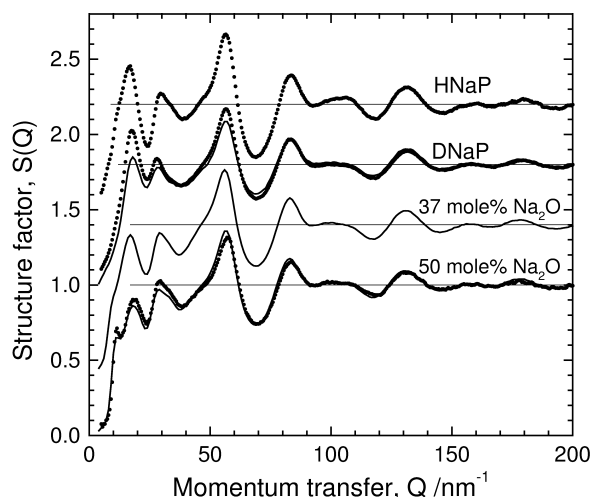


Fig. 1. Structure factors, $S(Q)$, of the hydrogenated and deuterated $\text{H}_2\text{O}-\text{Na}_2\text{O}-2\text{P}_2\text{O}_5$ glasses (HNaP, DNaP) and of two $(\text{Na}_2\text{O})_X-(\text{P}_2\text{O}_5)_{1-X}$ glasses with Na_2O fractions indicated in the plot. Data obtained from the SANDALS instrument are given with dotted lines. The LAD data are given with solid lines. Results of the $(\text{Na}_2\text{O})_X-(\text{P}_2\text{O}_5)_{1-X}$ glasses are already reported in [13].

two anhydrous sodium phosphate glasses. Data obtained at SANDALS are given with dotted lines and data obtained at LAD are given with solid lines. The SANDALS and LAD $S(Q)$ data of the 50 mole% Na_2O sample are nearly identical. The corresponding data of the DNaP sample differ in the height of the first diffraction peak. Note, the Q -ranges of the first detector groups are small, and an independent calibration according to $(d\sigma/d\Omega)_{\text{self}}$ is difficult. Mostly, fits are made to the data of detector groups with greater scattering angles which bears another uncertainty. Useful SANDALS data exist up to Q_{max} of $\sim 300 \text{ nm}^{-1}$, while LAD data are useful up to $\sim 550 \text{ nm}^{-1}$ [13]. The correlation functions, $T(r)$, of the HNaP and DNaP samples and of the anhydrous phosphate glasses are obtained by Fourier transformation (FT) using Q_{max} of 300 or 500 nm^{-1} with

$$T(r) = 4\pi r \rho_0 + 2/\pi \int_0^{Q_{\text{max}}} Q \cdot [S(Q) - 1] \sin(Qr) dQ, \quad (3)$$

where ρ_0 is the number density of atoms. The corresponding results are shown in Figs. 2 and 3. $T(r)$ functions obtained with Q_{max} of 500 (thin lines) and 300 nm^{-1} (thick lines) are compared for the anhydrous $\text{Na}_2\text{O}-\text{P}_2\text{O}_5$ glasses and sample DNaP (Figure 2). Split P–O peaks with resolved lengths of P–O_T

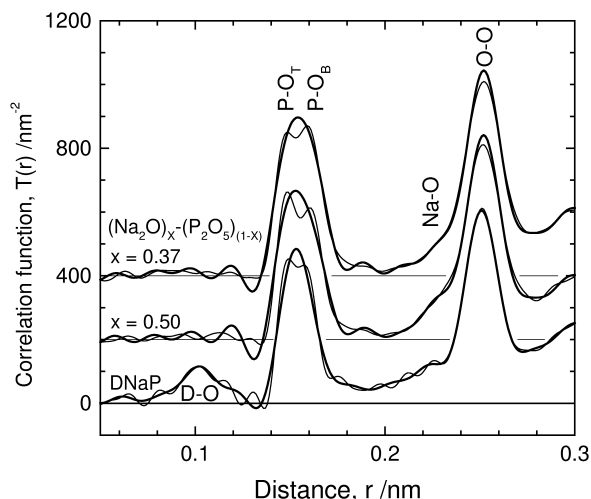


Fig. 2. Real-space correlation functions, $T(r)$, of the two $(\text{Na}_2\text{O})_X-(\text{P}_2\text{O}_5)_{1-X}$ glasses and the DNaP sample calculated from the LAD data using Q_{max} of 500 nm^{-1} (thin lines) and 300 nm^{-1} (thick lines).

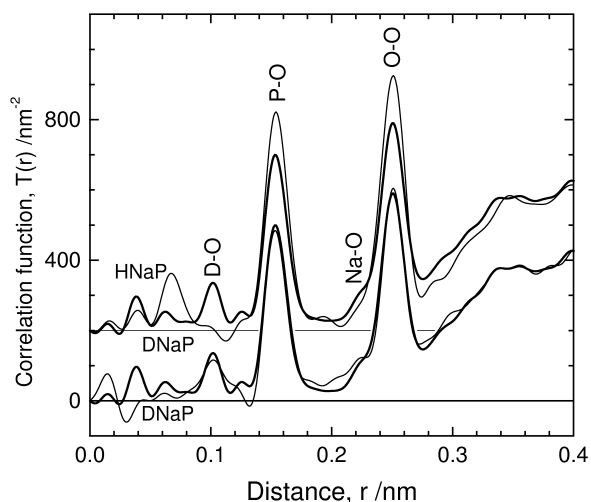


Fig. 3. Real-space correlation functions, $T(r)$, of the two $\text{H}_2\text{O}-\text{Na}_2\text{O}-2\text{P}_2\text{O}_5$ glasses obtained using $Q_{\text{max}} = 300 \text{ nm}^{-1}$. Upper functions: Comparison of the $T(r)$ functions of the hydrogenated HNaP (thin line) and deuterated DNaP (thick line) samples obtained from SANDALS data. Lower functions: Comparison of the $T(r)$ data of the DNaP sample obtained from SANDALS data (thick line) and LAD data (thin line).

and P–O_B bonds are visible if $Q_{\text{max}} = 500 \text{ nm}^{-1}$ is used, but not with $Q_{\text{max}} = 300 \text{ nm}^{-1}$ which is possible on SANDALS. O_T and O_B denote the terminal and bridging oxygen sites. The P–O and O–O peaks belonging to the PO_4 tetrahedra dominate the $T(r)$ functions also for the HNaP and DNaP samples (Figure 3).

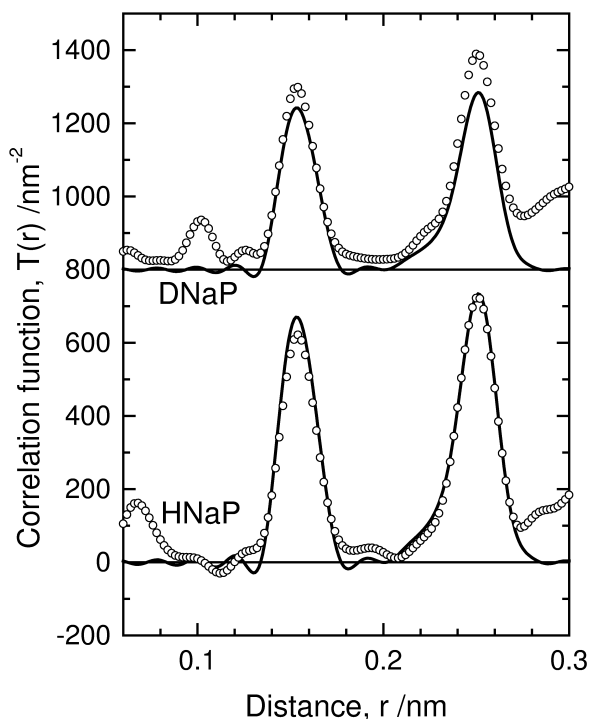


Fig. 4. Comparison of experimental (open circles) with model (solid line) $T(r)$ data for the DNaP and HNaP samples. The model functions are calculated using parameters obtained for the anhydrous NaPO_3 glass [13, 14].

The peak of the covalent H–O bonds is visible in the $T(r)$ data of the DNaP glass. The negative peak ($b_{\text{H}} = -3.74$ fm), expected at the same position for the HNaP sample, is not found. The $T(r)$ functions of the DNaP glass, obtained from SANDALS and LAD scattering data, are compared in the lower part of the figure. The differences are small.

At first it is examined to which extent the first neighbour-peaks in the $T(r)$ functions of the DNaP and HNaP samples are formed of contributions from the PO_4 tetrahedra and from the oxygen environments of the Na^+ ions. Parameters of the P–O, Na–O and O–O peaks are taken from the fits of the corresponding peaks in the $T(r)$ data of the NaPO_3 glass (50 mole% Na_2O) [13, 14]. The corresponding model first-neighbour peaks are compared with the experimental $T(r)$ of the DNaP and HNaP samples (cf. Fig. 4). Gaussian functions with the three parameters mean distance, coordination number and full width at half maximum (fwhm) are used to model the pair peaks. The Gaussian functions are convoluted with peak functions for taking into account the termination

effects caused by Q_{max} in FT (3) and are weighted according to the actual glass compositions. The FT termination causes an additional broadening of pair peaks and spurious satellite ripples, the effects of which are simulated by the method described in [15]. The peaks compared in Fig. 4 are almost at the expected positions, but the peak heights do not agree in all cases. The differences should be due to distances with H or D atoms longer than the length of the covalent D–O bonds which are visible as that peak at ~ 0.10 nm.

The next possible approach is the use of the first-order difference technique based on the H/D-contrast variation, where a difference $\Delta S(Q)$ function is calculated with

$$\Delta S(Q) = (S_{\text{D}}(Q) - 1) - 0.659(S_{\text{H}}(Q) - 1), \quad (4)$$

and the corresponding Fourier transform is analysed. The factor 0.659 is the quotient of the average scattering lengths of the HNaP and DNaP samples. The total $S(Q)$ factors are superpositions of ten partial $S_{ij}(Q)$ factors with i, j being the atomic species H(D), Na, P, and O. The weighting factors w_{ij} of the $S_{ij}(Q)$ in the total $S(Q)$ data are

$$w_{ij} = (2 - \delta_{ij})c_i c_j b_i b_j / \langle b \rangle, \quad (5)$$

where δ_{ij} is zero for $i \neq j$, otherwise it is unity. Since, except of b_{H} and b_{D} , the c_i , c_j , b_i , and b_j do not change for the samples HNaP and DNaP, the difference $\Delta S(Q)$ function is free of factors not containing b_{H} or b_{D} . So only four partial $S_{ij}(Q)$ factors are relevant for $\Delta S(Q)$:

$$\Delta S(Q) = 0.236S_{\text{HO}}(Q) + 0.070S_{\text{HP}}(Q) + 0.025S_{\text{HNa}}(Q) + 0.019S_{\text{HH}}(Q) - 0.35. \quad (6)$$

The resulting $\Delta S(Q)$ data are shown in the insert of Fig. 5, while the difference pair correlation, $\Delta g(r)$, fills the main part of this figure [$g(r) = T(r)/4\pi r\rho_0$]. A huge peak of covalent H–O bonds is found at ~ 0.10 nm, similar to the results of [11]. Also narrow but smaller peaks in $\Delta g(r)$ are found at ~ 0.15 and ~ 0.25 nm. They are interpreted as residuals of the P–O and O–O peaks whose formation dominates the $S_{\text{H}}(Q)$ and $S_{\text{D}}(Q)$ functions. The appearance of these small peaks is due to some correction and normalization deficits. Also other but broad contributions exist for distances smaller than 0.3 nm, which we attribute to H–O, H–P and H–Na pairs. For example, lengths of ~ 0.16 nm could belong to the hydrogen bond in

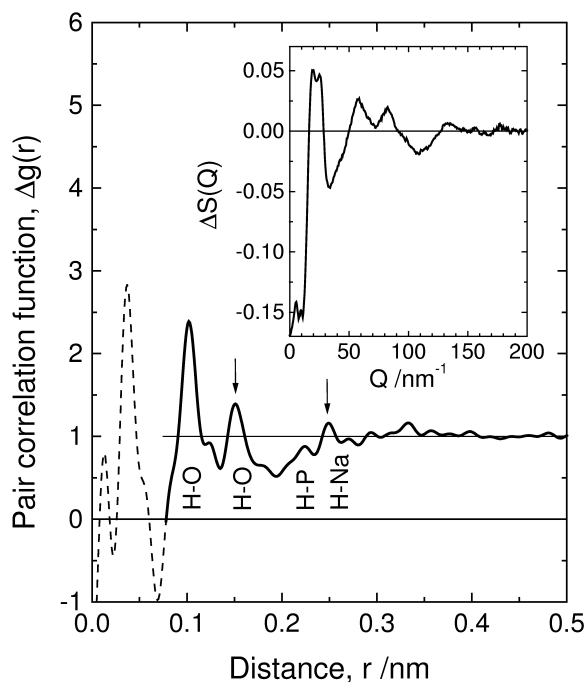


Fig. 5. Pair correlation function, $\Delta g(r)$, of $\text{H}_2\text{O}-\text{Na}_2\text{O}-2\text{P}_2\text{O}_5$ glasses obtained from an appropriate difference $\Delta S(Q)$ of the structure factors of samples DNaP and HNaP according to (4) which finally contains only the H–O, H–P, H–Na and H–H distances according to (6). The $\Delta S(Q)$ function is shown in the insert. Arrows mark residuals of the P–O and O–O peaks which appear due to minor normalization deficiencies.

the O–H···O hydrogen bridges. Fits of these contributions follow below. They are made to the $T(r)$ data of the HNaP and DNaP samples simultaneously, but not to the $\Delta g(r)$ function.

The first step of the fits is the search for reasonable starting parameters. A good approach is the use of structural parameters from related crystals, which here are the $\text{Na}_2\text{HP}_3\text{O}_9$ poly- [4] and cyclophosphates [5] having chemical compositions similar to that of the glasses studied. Also the structure of an $\text{Na}_2\text{H}_2\text{P}_4\text{O}_{12}$ crystal is reported [16], but H positions are not given and some disorder in the occupation of sites was found. Figure 6 shows a scheme of the hydrogen bridge with the next-nearest P and Na atoms as it exists in the cyclophosphate [5]. The H–O, H–P, H–Na, and O–O lengths given in Fig. 6, together with parameters of the P–O, Na–O and O–O peaks used above (cf. Fig. 4) are taken to calculate the model $T(r)$ functions. The results are compared in Figure 7. The cyclophosphate structure [5] yields a better fit than the

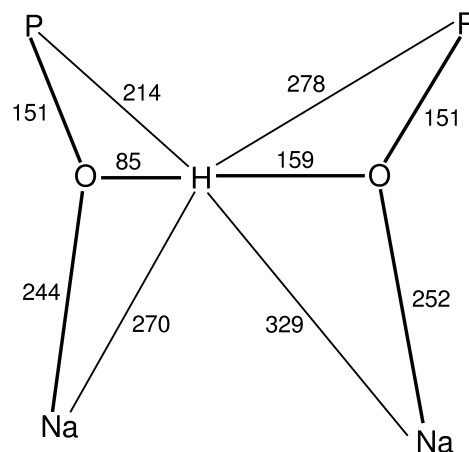


Fig. 6. Scheme of the hydrogen bridge in the $\text{Na}_2\text{HP}_3\text{O}_9$ tri-cyclophosphate crystal [5]. Distances are given in pm.

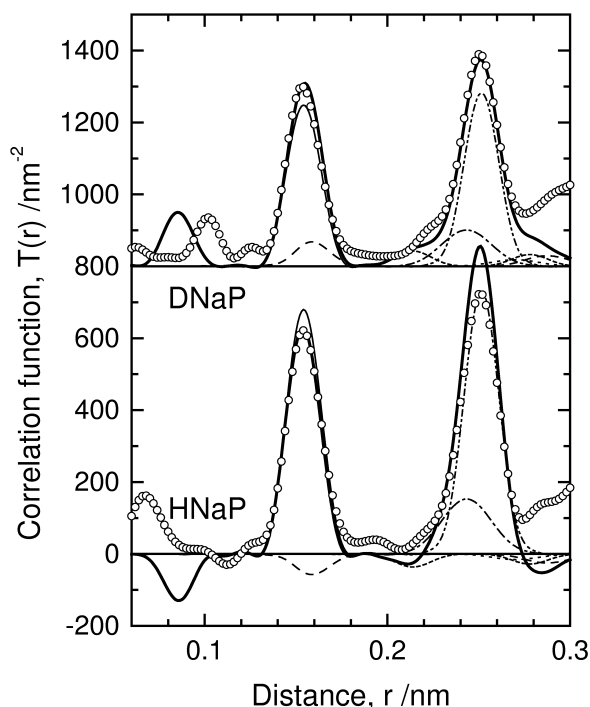


Fig. 7. Comparison of experimental (open circles) with model (thick solid line) $T(r)$ data for the DNaP and HNaP samples. The model functions are calculated using the distances taken from the $\text{Na}_2\text{HP}_3\text{O}_9$ tricyclophosphate crystal [5]. Peak widths are adjusted to give a good fit. The partial contributions are given with thin lines: H–O dashed line, P–O solid line, Na–O dash-single-dot line, O–O dash-double-dot line, H–P short-dashed line, Na–O even shorter dashed line.

polyphosphate. But the H–O length of 0.085 nm, reported for $\text{Na}_2\text{HP}_3\text{O}_9$ [5], is too short. The peaks at

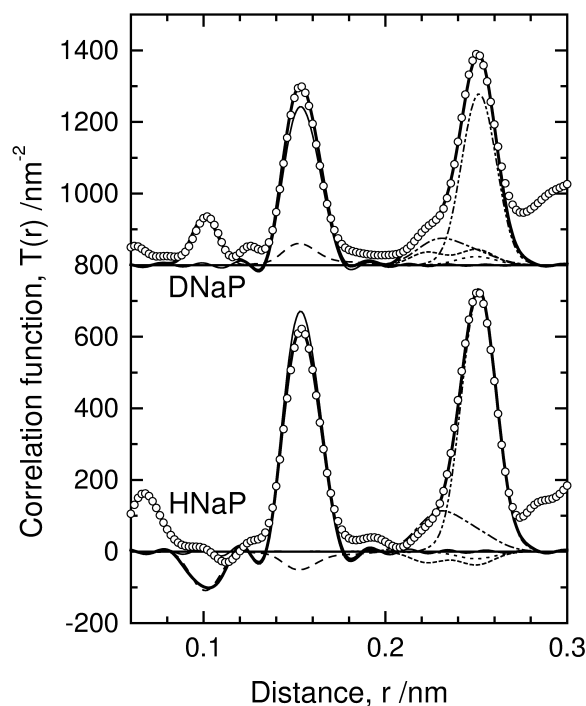


Fig. 8. Comparison of experimental (open circles) with model (thick solid line) $T(r)$ data for the DNaP and HNaP samples. The model functions are obtained by optimization of distances and peak widths starting from the parameters used for Figure 7. The partial contributions are given with thin lines: H–O dashed line, P–O solid line, Na–O dash-single-dot line, O–O dash-double-dot line, H–P short-dashed line, Na–O even shorter dashed line.

0.15 nm are well fitted due to the longer H–O distance in the hydrogen bridge whose contribution is positive for the DNaP and negative for the HNaP sample. But the model peak for the HNaP sample at 0.25 nm is too high if compared with the experimental result, while the same peak for DNaP is well fitted.

Subsequently, the fit of both $T(r)$ functions is improved by systematically adjusting some of the parameters, which is required especially for the distances in the range of the O–O peak at 0.25 nm. Least-squares fitting with independent parameters of all possible pair distances in the r -range up to 0.27 nm is not feasible. Subtle changes of the parameters of the pair peaks used before are made. The resulting model $T(r)$ functions are compared in Figure 8. The final parameters used are given in Table 1. Parameters of the two P–O distances could not be extracted from the fits but are those taken from [5, 13]. A separate determination of them, using the LAD $T(r)$ data, was not made for the DNaP sample (cf. Fig. 2). Due to poor statistics in the

Table 1. Parameters of the Gaussian functions used in fits of the first-neighbour peaks simultaneously made to the neutron correlation functions, $T(r)$, of the DNaP and HNaP samples. The coordination numbers marked with asterisks are fixed under the assumption that PO_4 tetrahedra are twofold-connected and each H atom forms a hydrogen bridge. The corresponding fit results are shown in Figure 8.

Atom pair	Coordination number	Distance (nm)	fwhm (nm)	Total coordination number	Mean distance (nm)
H(D)–O	1.00	0.101(2)	0.018(4)	1.0*	0.101
	0.85	0.153(2)	0.022(5)	1.0*	0.157
	0.15	0.180(10)	0.022(5)		
P–O	2.00	0.1486(10)	0.012(2)	4.0*	0.155
	2.00	0.1609(10)	0.013(2)		
Na–O	3.00(10)	0.228(3)	0.027(4)	5.0(5)	0.193
	2.00(10)	0.248(5)	0.030(5)		
O–O	4.33	0.2515(10)	0.022(3)	4.33*	
H(D)–P	0.80	0.223(5)	0.021(4)	2.0*	
	1.20	0.250(5)	0.023(4)		
H(D)–Na	1.00	0.250	0.025	1.0*	

high- Q range of the corresponding measurement some unphysical oscillations cannot be avoided. The O–O coordination number which considers the number of tetrahedral edges seen from a given O site is four at the metaphosphate composition. The additional part to N_{OO} of 0.33 (cf. Table 1) takes into account the O–O distances of the hydrogen bridges. The most evident change to the last fit we made is the reduction of the Na–O coordination number from six as in the crystal [5] to five for the glass. The O–H...O hydrogen bridges in the glass with participating H–O distances of 0.101 and 0.157 nm are longer than those in the crystal [5] (cf. Fig. 6). The H position in the hydrogen bridge of the glass is little more symmetric. Mean H–P distances of 0.223 and 0.250 nm are found instead of 0.214 and 0.278 nm given for the $\text{Na}_2\text{HP}_3\text{O}_9$ cyclophosphate [5]. Different from the angles of 128° given for the crystal (Fig. 6) H–O–P angles of 123° and 109° are estimated for the glass. The comparison with the crystal structure should not be overestimated: The composition of the glass is different from that of the $\text{Na}_2\text{HP}_3\text{O}_9$ crystal. XRD results of the crystal structure exhibit some uncertainty in the determination of the H positions.

4. Discussion

Phosphate glasses rich in P_2O_5 or modified with cations of low electric field strength are highly sensitive to water attack. Details of the structural behaviour of the H_2O molecules (or H^+ ions) in the glassy network are still waiting for clarification. The results of our present experiments on H_2O – Na_2O – $2\text{P}_2\text{O}_5$ glasses

agree with a typical network-modifying role of H_2O , where the oxygen is used for rupturing a P–O–P bridge changing two threefold-connected PO_4 (Q^3) to twofold-connected PO_4 (Q^2) units. This behaviour was already suggested for glasses of similar compositions [3]. The H^+ ions bridge the O_T corners of two PO_4 tetrahedra, whereby they form a single covalent bond to one of the corners.

In general, the H/D-substitution in neutron scattering experiments is an excellent tool for studying structural details of the H^+ environments. The preparation of samples of identical compositions is well solved by melting the glasses in sealed ampoules. The combined analysis of hydrogenated and deuterated samples is made under the assumption of identical structural effects of H and D isotopes. But especially for the hydrogenated sample (HNaP) prepared with ordinary water the problematic inelasticity correction together with the huge background of incoherent scattering can cause normalization problems and other errors. The H–O peak at 0.10 nm, expected with a negative amplitude, is not detected for HNaP. The unphysical peak at 0.07 nm could not be suppressed by varying the correction parameters. Note, the internal distances of the PO_4 tetrahedra dominate the scattering information in the $S_\text{H}(Q)$ and $S_\text{D}(Q)$ factors, which makes difficult to extract the information of the H^+ environments. Earlier H/D substitution work on water effects in silicate glasses [11] gives only an analysis of the pair peaks for the deuterated sample. The difference $\Delta S(Q)$ function was calculated, where the H–O peak of short covalent bonds was reproduced in the resulting $\Delta g(r)$ function [11]. Here we make a further step of analysis: Reasonable information is extracted from the $S_\text{H}(Q)$ data of the hydrogenated HNaP sample, as well. A deficit is the missing peak of covalent H–O bonds. The combined analysis of the $T(r)$ functions of both samples, DNaP and HNaP, yields parameters confirming the existence of twofold-linked PO_4 units together with H^+ ions occupying positions in the O–H \cdots O bridges. Small deficiencies exist for distances of ~ 0.19 nm (cf. Fig. 7). Here some positive contributions are missing in both $T(r)$ functions. Such distances can belong either to atom pairs where non of the partners is a H(D) atom, or to H–H pairs.

The number of H–O bonds with lengths of 0.10 nm is not suitable for differentiation between H atoms existing in H_2O molecules or in OH-groups. Other arguments can be given for the dominance of the OH-groups: Significant fractions of short H–H distances

of ~ 0.155 nm, typical of H_2O molecules, do not exist. They would give additional positive contributions to the $T(r)$ functions in the range of the P–O peaks for both the DNaP and HNaP samples. Moreover, the existence of a H–P distance of ~ 0.22 nm (Table 1) indicates that the H atom approaches a PO_4 tetrahedron. The simplest explanation for this distance is the formation of an OH-group with an O_T corner of a PO_4 tetrahedron as shown in Figure 6. Taking into account these H–P distances allows to fit the $T(r)$ function in the distance range from 0.20 to 0.23 nm excellently (cf. Fig. 8). Minor fractions of H_2O molecules cannot be excluded by the diffraction results.

On the other hand, it was mentioned above that H–H distances could fill the small difference between model and experimental $T(r)$ functions at 0.19 nm (Fig. 8). Distances of this length might appear if two H^+ share an O_T corner of a PO_4 unit forming a $\text{H}\cdots\text{O}_\text{T}\cdots\text{H}$ link. Replacement of the left Na^+ shown in Fig. 6 by a H^+ ion with a H–O distance of 0.157 nm would result in the H–H distance of 0.19 nm. However, we assume that such distances are improbable and speculative. Sufficient O_T atoms are available to avoid short H–H distances with strong repulsive forces between the H^+ ions. Four O_T are available for each H atom. The shortest H–H distance in the crystal $\text{CaH}_2\text{P}_4\text{O}_{12}$ [6], it has the same $n(\text{O}_\text{T})/n(\text{H})$ ratio as the glass, is 0.37 nm. Even in the crystal structure of H_3PO_4 [17] with a ratio $n(\text{O}_\text{T})/n(\text{H})$ equal to 1.33 the shortest H–H distance is 0.24 nm, where two H atoms share an O_T corner with a $\text{H}\cdots\text{O}_\text{T}\cdots\text{H}$ link via two hydrogen bonds. Since we too do not find suitable distances other than H–H pairs, we attribute the deficiencies at 0.19 nm rather to some systematic error.

Figure 2 shows split P–O peaks for two anhydrous sodium phosphate glasses and the DNaP sample. A change of the fractions of the P– O_T and P– O_B bonds is visible in the P–O peaks of both anhydrous glasses, which is due to a change of composition [13]. In comparison with the NaPO_3 glass ($x = 0.5$), the DNaP sample shows similar fractions of P– O_T and P– O_B bonds. Here the numbers of P– O_T and P– O_B bonds are equal to each other, which is expected for the twofold-connected PO_4 units existing at metaphosphate composition. This fact confirms the network-modifying role of H_2O in ultraphosphate structures, such as was found by ^{31}P MAS NMR [3]. Another effect becomes obvious in Fig. 2: The decrease of the difference between the lengths of P– O_T and P– O_B bonds for the DNaP sample, where half of the Na^+ sites are

replaced by H^+ ions if compared with $NaPO_3$, follows the tendency found for other network-modifying ions [13]. The decrease of the difference of lengths is due to an increase of the electric field strength of the modifier ions [18, 19]. The same behaviour is found for the bond lengths of related crystal structures, e.g., for the tricyclopophosphates [5, 20]. The mean lengths of the $P-O_T$ and $P-O_B$ bonds in $Na_3P_3O_9$ [20] are 0.1484 and 0.1614 nm, while 0.1488 and 0.1610 nm are given for $Na_2HP_3O_9$ [5]. The mean lengths of the $P-O_T$ bonds of the latter crystal are 0.1507 or 0.1478 nm if those with the H^+ or only the Na^+ neighbours are considered separately [5]. The fits of the $T(r)$ data of the glasses studied were made under the assumption of two different $P-O$ bonds with starting parameters taken from the $Na_2HP_3O_9$ crystal [5]. The resulting bond lengths (0.1488 and 0.1610 nm) are little varied.

The oxygen environments of the Na^+ ions with $Na-O$ coordination numbers, N_{NaO} , of five agree with the situation found for the anhydrous glasses [14]. Every O_T is shared by two or three Na^+ neighbours. So an Na^+ site links up to five different PO_4 tetrahedra forming a spherical oxygen environment which contributes to the stiffness of the structure. Note, metaphosphate glasses possess only PO_4 chains (or some cyclic structures) which might have elastic properties similar to a polymer. But even alkali ions contribute to stiffness and structural stability. For example, an increase of the glass transition temperature T_g was found with increasing modifier fractions for Li and Na phosphate glasses [21]. The effect of H^+ ions is different. Corners of only two PO_4 units are connected by $O-H \cdots O$ bridges. The structure becomes more flexible. We prepared metaphosphate glasses where the full Na^+ fraction was replaced by H^+ ions. The corresponding material could not be crushed as a usual oxide glass, but it possesses clear elasticity. However, glass structures containing hydrogen are still densely packed. A hydrogen bridge is comparably short with an $O-O$ distance being equal to the edge length of a PO_4 tetrahedron.

Also these lengths were taken into account when calculating the $O-O$ coordination number of 4.33 given in Table 1. The number density of atoms of the $NaPO_3$ glass (74 nm^{-3}) [14] is less than that of the $HNaP$ glass studied (80.5 nm^{-3}), but it is similar if the number of H^+ ions is neglected (72.5 nm^{-3}). The water in the phosphate structures adapted as hydrogen bridges does not cause an opening of the glassy network.

5. Conclusions

Neutron diffraction with isotopic H/D -substitution was used to show the network-modifying effect of water in glassy ultraphosphate structures. The main effect is a rupture of $P-O-P$ bridges with H^+ ions forming $O-H \cdots O$ bridges connecting two corners of adjacent PO_4 units. So, instead of the specifics of a sodium ultraphosphate glass with interstitial water the character of a metaphosphate structure (equal fractions of $P-O_T$ and $P-O_B$ bonds) is developed with H_2O acting as a modifier oxide. Different from the spherical oxygen environments of other modifier ions, H^+ forms $O-H \cdots O$ bridges. The corresponding distances $H-O$ (0.101 and 0.157 nm) and $H-P$ (0.223 and 0.250 nm) are detected in a simultaneous analysis of the first-neighbour peaks of the $T(r)$ functions of the hydrogenated and deuterated $H_2O-Na_2O-2P_2O_5$ sample. The $O-O$ distances of the hydrogen bridges superpose with the edge lengths of the PO_4 tetrahedra, which leads to a rather dense packing. Fractions of short $H-H$ pair distances, typical of water molecules (0.155 nm) or clusters of hydrogen bridges, are not detected. The $Na-O$ coordination number of five is similar to that found for $NaPO_3$ glass.

Acknowledgements

Financial support of Deutsche Forschungsgemeinschaft (contract KR 1372/9-1) is gratefully acknowledged.

- [1] J. R. van Wazer, *Phosphorus and its Compounds* (vol. 1), Interscience, New York 1958.
- [2] K. Meyer, A. Barz, and D. Stachel, *J. Non-Cryst. Solids* **191**, 71 (1995).
- [3] R. K. Brow, R. J. Kirkpatrick, and G. L. Turner, *J. Non-Cryst. Solids* **116**, 39 (1990).
- [4] K. H. Jost, *Acta Crystallogr.* **15**, 951 (1962).
- [5] M. T. Averbuch-Pouchot, J. C. Guitel, and A. Durif, *Acta Crystallogr. C* **39**, 809 (1983).
- [6] M. T. Averbuch-Pouchot, *Z. Anorg. u. Allg. Chemie* **621**, 506 (1995).
- [7] A. Olbertz, D. Stachel, I. Svoboda, and H. Fuess, *Acta Crystallogr. C* **52**, 1603 (1996).
- [8] A. K. Soper, and A. Luzar, *J. Chem. Phys.* **97**, 1320 (1992).
- [9] V. F. Sears, in: *International Tables for Crystallography*, Vol. C (Ed. A. J. C. Wilson), Kluwer Academic, Dordrecht 1995, p 383.

- [10] A. K. Soper, IOP Conf. Series **97**, 354 (1989).
- [11] N. Zotov, H. Keppler, A. C. Hannon, and A. K. Soper, J. Non-Cryst. Solids **202**, 153 (1996).
- [12] A. C. Hannon, W. S. Howells, and A. K. Soper, IOP Conf. Ser. **107**, 193 (1990).
- [13] U. Hoppe, R. Kranold, D. Stachel, A. Barz, and A. C. Hannon, Z. Naturforsch. **55a**, 369 (2000).
- [14] U. Hoppe, D. Stachel, and D. Beyer, Phys. Scripta T **57**, 122 (1995).
- [15] R. L. Mozzi and B. E. Warren, J. Appl. Crystallogr. **2**, 164 (1969).
- [16] O. H. Jarchow, Acta Crystallogr. **17**, 1253 (1964).
- [17] R. H. Blessing, Acta Crystallogr. B **44**, 334 (1988).
- [18] T. Uchino, and Y. Ogata, J. Non-Cryst. Solids **191**, 56 (1995).
- [19] U. Hoppe, G. Walter, D. Stachel, and A. C. Hannon, Z. Naturforsch. **51a**, 179 (1996).
- [20] H. M. Ondik, Acta Crystallogr. **18**, 226 (1965).
- [21] J. J. Hudgens, R. K. Brow, D. R. Tallant, and S. W. Martin, J. Non-Cryst. Solids **223**, 21 (1998).